The Astrophysical Journal, 677:1268–1277, 2008 April 20

DISCOVERY OF A VERY BRIGHT, NEARBY GRAVITATIONAL MICROLENSING EVENT

B. Scott Gaudi,[1] Joseph Patterson,[2] David S. Spiegel,[2] Thomas Krajci,[3] R. Koff,[4] G. Pojmański,[5] Subo Dong,[1] Andrew Gould,[1] Jose L. Prieto,[1] Cullen H. Blake,[6] Peter W. A. Roming,[7] David P. Bennett,[8] Joshua S. Bloom,[9,10] David Boyd,[11] Michael E. Eyler,[12] Pierre de Ponthière,[13] N. Mirabal,[2] Christopher W. Morgan,[1,12] Ronald R. Remillard,[14] T. Vanmunster,[15] R. Mark Wagner,[16] and Linda C. Watson[1]

Received 2007 March 6; accepted 2008 January 10

ABSTRACT

We report the serendipitous detection of a very bright, very nearby microlensing event. In late 2006 October, an otherwise unremarkable A0 star at a distance of ∼1 kpc (GSC 3656−1328) brightened achromatically by a factor of nearly 40 over the span of several days and then decayed in an apparently symmetrical way. We present a light curve of the event based on optical photometry from the Center for Backyard Astrophysics and the All Sky Automated Survey, as well as near-infrared photometry from the Peters Automated Infrared Imaging Telescope. This light curve is well fit by a generic microlensing model. We also report optical spectra and *Swift* X-ray and UV observations that are consistent with the microlensing interpretation. We discuss and reject alternative explanations for this variability. The lens star is probably a low-mass star or brown dwarf, with a relatively high proper motion of $\gtrsim$20 mas yr^{-1}, and may be visible using precise optical/infrared imaging taken several years from now. A modest, all-sky survey telescope could detect ∼10 such events per year, which would enable searches for very low mass planetary companions to relatively nearby stars.

Subject headings: gravitational lensing — stars: individual (GSC 3656−1328)

Online material: color figures

1. INTRODUCTION

At the very moment in 1936 that he introduced[17] the concept of gravitational microlensing of one star by another closely aligned along its line of sight, Einstein famously dismissed its practical significance. Noting that the characteristic scale (what we now call the "Einstein radius") was extremely small, he concluded that "there is no great chance of observing this phenomenon, even if dazzling by the light of the much nearer star is disregarded" (Einstein 1936). It is easily shown that the optical depth to microlensing (the probability that any given star lies projected within the Einstein radius of another) is only about $\tau \sim 10^{-8}$ among the $V \leq 12$ stars that were typically cataloged in Einstein's day. As there are only a few million such stars altogether, the probability that any of these are microlensed at any given time is much less than 1 (Nemiroff 1998). Such a calculation may have influenced Einstein to resist the determined efforts by Hungarian engineer R. W. Mandl to get Einstein to publish his microlensing formulae and perhaps also to compose a letter to the editor of *Science* to "thank you for your cooperation with the little publication, which Mister Mandl squeezed out of me. It is of little value, but it makes the poor guy happy" (Renn et al. 1997).

Since Einstein's 1936 article, several authors have attempted to resurrect the idea of microlensing (e.g., Liebes 1964; Refsdal 1964). However, microlensing experiments did not actually get under way until the early 1990s (Alcock et al. 1993; Aubourg et al. 1993; Udalski et al. 1993). These experiments were motivated both by the suggestion of Paczyński (1986) to simultaneously monitor millions of stars in the dense star fields of nearby galaxies and by contemporaneous advances in technology that made such experiments feasible.

To date, several thousand microlensing events have been discovered toward several lines of sight, including the Large and Small Magellanic Clouds (Alcock et al. 1997, 2000; Palanque-Delabrouille

[1] Department of Astronomy, The Ohio State University, 140 West 18th Avenue, Columbus, OH 43210; gaudi@astronomy.ohio-state.edu.
[2] Department of Astronomy, Columbia University, 550 West 120th Street, New York, NY 10027.
[3] Center for Backyard Astrophysics (New Mexico), 9605 Goldenrod Circle, Albuquerque, NM 87116.
[4] Center for Backyard Astrophysics (Colorado), Antelope Hills Observatory, 980 Antelope Drive West, Bennett, CO 80102.
[5] Warsaw University Astronomical Observatory, Al. Ujazdowskie 4, 00-478 Warszawa, Poland.
[6] Harvard-Smithsonian Center for Astrophysics, 60 Garden Street, Cambridge, MA 02138.
[7] Department of Astronomy and Astrophysics, Pennsylvania State University, 525 Davey Lab, University Park, PA 16802.
[8] Department of Physics, University of Notre Dame, Notre Dame, IN 46556.
[9] Department of Astronomy, University of California, 601 Campbell Hall, Berkeley, CA 94720-3411.
[10] Sloan Research Fellow.
[11] Center for Backyard Astrophysics (England), 5 Silver Lane, West Challow, Wantage OX12 9TX, UK.
[12] Department of Physics, United States Naval Academy, 572C Holloway Road, Annapolis, MD 21402.
[13] Center for Backyard Astrophysics (Lesve), 15 rue Pré Mathy, 5170 Lesve (Profondeville), Belgium.
[14] Kavli Institute for Astrophysics and Space Research, Massachusetts Institute of Technology, 77 Massachusetts Avenue, Cambridge, MA 02139-4307.
[15] Center for Backyard Astrophysics (Belgium), Belgium Observatory, Walhostraat 1A, B-3401 Landen, Belgium.
[16] Large Binocular Telescope Observatory, University of Arizona, 933 North Cherry Avenue, Tucson, AZ 85721.
[17] There is some confusion as to who first worked out the basic concepts of gravitational microlensing. Indeed, Eddington (1920) and Chwolson (1924) both discussed the possibility in the 1920s. However, further research has shown that Einstein had already worked out the basic formalism of microlensing in 1912 (Renn et al. 1997), modulo the famous "factor of 2" increase in the deflection of light that he only discovered when he introduced general relativity 4 years later. In fact, Soldner (1804) derived the classical value for the deflection of light by a massive body over 100 years before Einstein, although he did not consider the associated magnification of the source by the lens. See Schneider et al. (1992) for a more thorough discussion of the history of gravitational lensing.

et al. 1998), as well as M31 (Paulin-Henriksson et al. 2002; de Jong et al. 2004; Uglesich et al. 2004; Calchi Novati et al. 2005). However, the vast majority of events have been detected toward the Galactic bulge (Udalski et al. 2000; Thomas et al. 2005; Hamadache et al. 2006) or fields in the Galactic plane relatively close to the bulge (Derue et al. 2001). The source stars of these events have generally been relatively faint, $V \gtrsim 15$. In these cases, the optical depth is of order 10^{-6}, i.e., 100 times higher than for the local stars that Einstein would have considered because the targets are about 10 times farther away. The larger distance makes the area of the Einstein ring about 10 times bigger and increases the column density of potential lenses by another factor of 10.

In the intervening years since the first microlensing events were discovered, a few authors have revisited the idea of detecting bright and/or nearby microlensing events. Colley & Gott (1995) argued that microlensing events visible to the naked eye are exceedingly rare, occurring at a rate of one per 40,000 yr for lensing by known stars. Microlensing of fainter stars is obviously more common; the event rate for stars with $V \lesssim 15$ is roughly one per year (Nemiroff 1998; Han 2007). This calculation led Nemiroff (1998) and Nemiroff & Rafert (1999) to point out that only small-aperture instruments are required to discover these brightest microlensing events, and that monitoring the entire sky down to $V \sim 15$ on relatively short timescales would soon be feasible. Di Stefano (2005) considered in detail a related idea of "mesolensing": microlensing of background stars by nearly lenses with large angular Einstein rings and large proper motions. Mesolensing can be used to study the properties of nearby stars, and in particular their planetary companions (Di Stefano 2008a, 2008b; Di Stefano & Night 2008). See § 4 for further discussion of the potential of microlensing to discover and study nearby planetary systems.

Although, given the typical source distances of ~8–50 kpc for microlensing searches toward the Galactic bulge and the Magellanic Clouds, the majority of the microlenses giving rise to observed events have been located at distances of a kiloparsec or more, there is nevertheless a low-probability tail of more nearby microlenses (Gould et al. 1994; Di Stefano 2005). Indeed, there is one event for which the lens has been robustly located to within a kiloparsec of the Sun, MACHO-LMC-5 (Alcock et al. 2001; Gould et al. 2004). Another event, EROS2-LMC-8, is also likely due to a nearby microlens, although this has yet to be confirmed with follow-up observations (J. P. Beaulieu 2008, private communication; see also Tisserand & Milsztajn 2004 and Tisserand et al. 2007). Thus, nearby lenses can be uncovered and studied in ongoing surveys. However, these surveys are not very efficient at discovering nearby microlenses; furthermore, the source stars of these events are necessarily faint, making detailed monitoring and follow-up observations difficult.

Here we report on a microlensing event of the type Einstein believed would never be observed: a magnification $A = 40$ event of the $V \sim 11.4$ A-type star GSC 3656−1328, located about 1 kpc from the Sun in the disk of the Milky Way. Although such events are indeed quite rare, microlensing of somewhat fainter nearby stars occurs with reasonable frequency. While this event was found serendipitously, we argue that with recent technological advances it is now feasible to monitor the sky to deliberately and routinely detect these "domestic" microlensing events. We propose a telescope design to accomplish this, and we argue that it is possible to build two copies of such a telescope that could monitor the majority of the sky down to $V \sim 16$ at modest cost. Monitoring of the discovered microlensing events would enable a novel method to detect nearby planets, allow a search for dark objects in the Milky Way disk, and permit several days' advance warning for potentially hazardous asteroid impacts.

Fukui et al. (2007) also report on observations of the transient event in GSC 3656−1328. A subset of the data presented here is in common with theirs; however, the analyses were done completely independently. They also conclude that the brightening seen in GSC 3656−1328 is likely due to microlensing.

2. OBSERVATIONS

On 2006 October 31, A. Tago announced a sudden brightening in the close vicinity of GSC 3656−1328 (Nakano & Tago 2006; Nakano et al. 2006), a $V = 11.4$ A0 V–A1 V star[18] ~8° from the Galactic plane in Cassiopeia with a distance of ~1 kpc. Confirmation followed a few hours later in the variable star newsgroups; this established that the star was in fact the source of the brightening and roughly measured the amount and timescale of the brightening (to $V = 7.5$, rising in about a week).

We began our photometry with the small telescopes of the Center for Backyard Astrophysics (CBA; Skillman & Patterson 1993) on November 1 (=JD′ = JD − 2,450,000 = 4040) and found the star at $V = 8.9$, falling rapidly and smoothly, with no additional variability at the few percent level. In the next few days, we obtained time-series and multicolor photometry with CBA telescopes, spectroscopy with the MDM 2.4 m telescope, and a pointed 5000 s X-ray observation with *Swift* (Gehrels et al. 2004) using the X-ray telescope (Burrows et al. 2005); we also searched for X-ray outbursts over the 10 yr lifetime of the All-Sky Monitor aboard *RXTE*. The basic conclusion from all of these observations was simple: the star had brightened by 4 mag, but with no change in spectrum or color ($B - V = 0.2$), no flickering, and no discernible X-ray signature (with a *Swift* upper limit in the 0.5–10 keV band of $<4 \times 10^{-13}$ ergs cm^{-2} s^{-1}). A search of 400 photographic plates during 1964–1994 showed no variability in the star (Samus & Antipin 2006), and we found no X-ray outbursts from this position.

This seemed unlike any known type of intrinsic variable star, and several reports suggested instead that GSC 3656−1328 may have microlensed by an intervening passing star (Mikolajewski et al. 2006a, 2006b; Spiegel 2006). After 2 weeks of data, our preliminary fit of the light curve to a microlens model (see § 3) seemed promising. However, there were only a few very uncertain measurements (with typical errors of ±0.4 mag) before the peak, and identifying microlensing events based on falling-only light curves can be problematic (Smith 2003; Afonso et al. 2006). Given the low a priori likelihood for such a nearby star to be microlensed, we eagerly sought additional data to confirm (or refute) the microlensing interpretation. In particular, we sought data before the apparent peak on October 31, as well as data covering a wide baseline in wavelength, in order to ascertain whether the variation was both symmetric about the peak and achromatic, as would generally be expected for a short microlensing event of an isolated star.

We were fortunate to find 15 images of the field in the V and I bands in the test runs of the northern (Hawaii) station of the All Sky Automated Survey (ASAS; the southern station is described by Pojmański 2004). These images have errors of ±0.04 mag, cover (although sparsely) the rise of the event, and fortuitously include one I-band measurement obtained almost exactly at the peak, judged by a microlensing fit to the remainder of the data set, as described below. Since ASAS-North had just begun operation, this was mighty lucky.

As for wavelength coverage, we supplemented the CBA monitoring with four epochs of UV observations (on JD′ = 4042,

[18] We summarize the properties of GSC 3656−1328 in Appendix A.

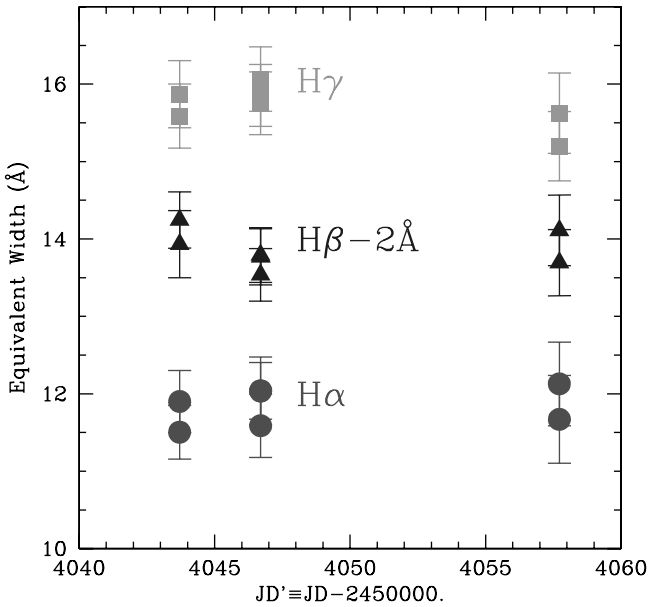

FIG. 1.—EWs of the Hα (*circles*), Hβ (*triangles*), and Hγ (*squares*) lines of GSC 3656−1328 as a function of JD − 2,450,000. The measurements for Hβ have been offset by 2 Å for clarity, as indicated. The broadband optical photometry in Fig. 2 demonstrates that during the time span between the first and last spectroscopic measurements, the continuum flux of GSC 3656−1328 decreased by a factor of ∼2, whereas the EWs of Hα, Hβ, and Hγ remained constant to within the uncertainties. [*See the electronic edition of the Journal for a color version of this figure.*]

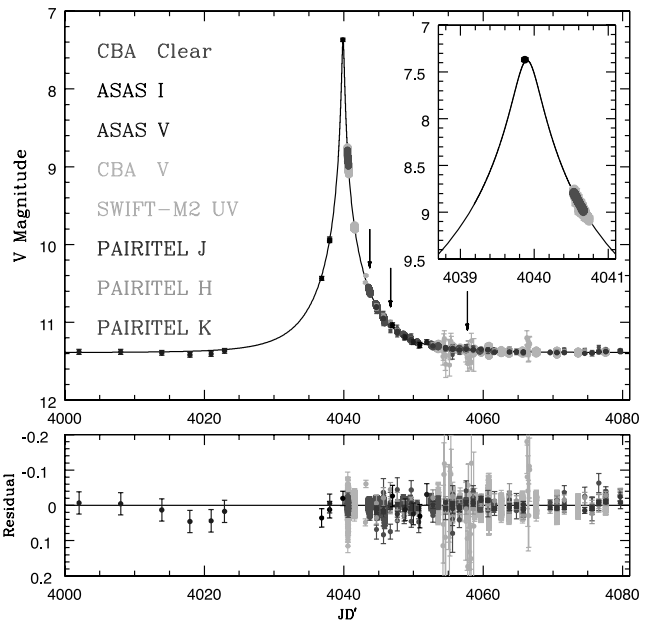

FIG. 2.—Data and residuals from a microlensing model fit to the UV, optical, and IR photometry of GSC 3656−1328. *Top*: Symbols with error bars show photometry from CBA clear and *V*; ASAS *I* and *V*; *Swift* M2; and PAIRITEL *J*, *H*, and K_s as a function of JD′ = JD − 2,450,000. All data except for the ASAS *I* and *V* bands have been aligned to the CBA *V* band by subtracting a constant magnitude offset. For the ASAS data, the additional contribution from unresolved neighboring stars has been removed using the microlensing model fit. See the text for details. The solid line shows the best-fit microlensing model. The arrows show the epochs of the spectroscopic measurements. The inset shows a detail near the peak of the event. *Bottom*: Residuals from the best-fit microlensing model. The achromatic and symmetric variability of GSC 3656−1328 is well fit by a microlensing model. [*See the electronic edition of the Journal for a color version of this figure.*]

4055, 4057, and 4067) using the UVOT camera on *Swift* (Roming et al. 2005) and a long program of infrared monitoring from the Peters Automated Infrared Imaging Telescope (PAIRITEL; Bloom et al. 2006) on Mount Hopkins. PAIRITEL is a 1.3 m telescope equipped with the former 2MASS (Skrutskie et al. 2006) camera that simultaneously images the near-infrared JHK_s bands. We obtained ∼1500 7.8 s images in each band nearly every night from program start (JD′ = 4044) until the event returned to baseline. Since the variations were smooth, we binned the images into 51 separate epochs, and the magnitude of the source at each epoch was determined using differential aperture photometry against a set of reference stars from the 2MASS catalog. The *Swift* UV data from this bright source were strongly affected by coincidence losses, and to minimize these we used only the M2 band (centered on 2400 Å) and estimated the flux of the source by summing in an annulus centered on the source, with an inner radius of 12″ and an outer radius of 20″.

We also obtained seven optical spectra using the CCDS instrument on the MDM 2.4 m telescope on Kitt Peak, two near JD′ ∼ 4043.7, three near ∼4046.7, and two near ∼4057.7. The spectra cover 4000−6800 Å, with a resolution of ∼15 Å FWHM, as measured from arc-lamp lines. They reveal an unremarkable early A star, showing prominent resolved (FWHM ∼ 25 Å) Balmer lines. We measured the equivalent widths (EWs) of Hα, Hβ, and Hγ in each spectrum by integrating over a window of ±60 Å, fitting a third-order polynomial to estimate the local continuum. We estimated the uncertainties in the EW measurements by generating a series of mock spectra with identical noise properties and measuring the EWs in these spectra in the same manner as the actual data. See Figure 1.

3. MICROLENSING INTERPRETATION

Figure 2 shows the collected UV, optical, and near-IR photometry of GSC 3656−1328 during the transient variability. For all of these data except those from the CBA, the photometric uncertainties are due to the photon noise from the source and comparison stars. In the case of the CBA data sets, we estimated the uncertainties to be equal to the rms variability about a linear fit to the time-series data on the first night (JD′ = 4040). We align all of the bands to the CBA *V* band by subtracting a constant magnitude offset, except for the ASAS data, which due to the larger point-spread function (PSF) and photometric aperture include an additional contribution from unresolved neighboring stars. In this case, we remove this unresolved ("blended") light using the microlensing model fit, as described below. The baseline magnitude of the microlensing source determined in this way is consistent with that measured directly from higher resolution images. As is evident from Figure 2, the variability is essentially achromatic (i.e., the color of the event is constant) over nearly a decade in wavelength. Furthermore, although the sampling on the rising side of the event is sparse, the variability is apparently symmetric about the time of peak brightness near JD′ ≃ 4040.

Our spectra show no evidence for any emission features and are completely consistent with that of a normal A0 V star. Furthermore, there is no evidence for any change in the spectrum of the star between JD′ ≃ 4043.7 and 4057.7, during which time the continuum flux decreased by a factor of ∼2. This can be quantified by the EWs of the Balmer lines, which were constant to within the measurement uncertainties (typically 2%−4%) during this period (see Fig. 1). Reports of optical spectra taken by other groups, which span a broader range of epochs, apparently confirm this lack of spectral evolution (Munari et al. 2006; Mikolajewski et al. 2006a, 2006b). The target-of-opportunity observation by the *Swift* satellite showed no detectable X-ray emission, as would be expected from outbursting variables.

These characteristics of the variability in GSC 3656−1328, namely, the precise light-curve shape including the apparent symmetry about the peak, achromaticity, and lack of emission features or changes in the absorption features, are expected for microlensing but would be very unusual for outbursting variable stars, which generally change temperature (and therefore color) during explosive outbursts. Essentially, what is required to reproduce the type of variability seen in GSC 3656−1328 is for the angular size of the star to change by a factor of $\sim(40)^{1/2} \sim 6$ while the temperature remains constant to $\lesssim$5%. The only way for this to occur is for the apparent area of the star to change, as occurs in a microlensing event. Occultation of the star due to, e.g., an eclipsing binary companion can also make such a change in the apparent area, but obviously in this case one would expect a dimming, not the brightening that is observed here.

When microlensing surveys were first being planned, a major concern was the potential contamination from intrinsic stellar variability. As a result, a number of studies addressed the question of whether there exists a class of variable stars whose variability might be misinterpreted as microlensing. At least two types of potential contaminants were identified.

"Blue bumpers" are blue main-sequence stars whose fluxes remain constant for long periods of time but occasionally undergo brightenings ("bumps") that are approximately symmetric about the peak and have durations that are consistent with the expectations for microlensing events (Cook et al. 1995; Alcock et al. 1996, 2000). However, closer inspection reveals that these variables have properties that can be used to exclude them as the explanation for the variability seen in GSC 3656−1328. First, many or perhaps all of these variables are Be-type stars, exhibiting Balmer line emission (Cook et al. 1995). Second, the brightenings are exclusively low-amplitude, with peak brightenings of less than 1.5 times the baseline flux (Alcock et al. 2000). Finally, detailed light curves typically show slight asymmetries (Cook et al. 1995; Alcock et al. 2000).

At least some dwarf nova (DN) outbursts are characterized by approximately symmetric brightenings with amplitudes and durations that are consistent with that seen in GSC 3656−132 (della Valle 1994; Beaulieu et al. 1995; della Valle & Livio 1996). However, it is unlikely that the GSC 3656−132 variability is due to a DN outburst. First, spectra of DNs typically exhibit H or He emission (della Valle 1994; Beaulieu et al. 1995). Second, while the light curves of novae have properties that are grossly similar to microlensing events, they do not follow the standard Paczyński (1986) form at the ∼2% level with which the GSC 3656−1328 variability has been measured (e.g., Smith 2003; Afonso et al. 2006). Finally, the interval between outbursts of DNs is known to be directly related to the strength of the outburst, such that larger outbursts generally have longer intervals between outbursts (Smak 1984; van Paradijs 1985). DN outbursts with amplitudes similar to the brightening seen in GSC 3656−132 would be expected to have average recurrence times of tens to hundreds of days (van Paradijs 1985). It seems unlikely that the kinds of observations that originally discovered the variability discussed here (e.g., Nakano & Tago 2006; Nakano et al. 2006) would have missed previous outbursts; furthermore, there is no evidence for such outbursts in the photographic plate observations taken during 1964–1994 (Samus & Antipin 2006). Regardless, continued monitoring of GSC 3656−1328 would certainly allow one to rule out the DN hypothesis definitively.

It is interesting to note that the source stars of the first two EROS microlensing event candidates (Aubourg et al. 1993) are both early-type main-sequence stars. Spectroscopic observations showed that the source of EROS-LMC-1 is a Be star with Balmer emission lines, whereas the source of EROS-LMC-2 is a seemingly normal A0 main-sequence star with no apparent emission lines (Beaulieu et al. 1995). However, EROS-LMC-2 also exhibits periodic variability with an amplitude of ∼0.5 mag and a period of ∼2.8 days, indicative of an eclipsing binary (Ansari et al. 1995). In both cases, continued photometric monitoring of the source stars revealed additional brightenings many years later, with amplitudes and timescales similar to those of the original events (Lasserre et al. 2000; Tisserand et al. 2007), thus excluding the microlensing interpretation of the variability.

Given the evidence in favor of microlensing, we first test whether the UV, optical, and IR data can be acceptably fit to a simple microlensing model. This model has as parameters the Einstein timescale $t_{\rm E}$, the impact parameter (closest source-lens approach in units of the angular Einstein radius $\theta_{\rm E}$) u_0, and the time-of-maximum magnification t_0. In addition, we fit for the baseline flux of the lensed source for each of the eight separate observatory/filter combinations. Since we expect any light in the PSF to be completely dominated by the bright source, we do not allow for any flux that is blended with the source but is not microlensed, with the exception of the ASAS data, which are known to contain light from unresolved stars in the photometric aperture. Thus, this model has $3 + 7 + 2 = 12$ parameters. This best-fit model is shown in Figure 2. We find that the microlensing model provides a reasonable fit to the data: the χ^2/dof for the individual data sets ranges from ∼0.8 for 2802 data points for the CBA V data set to ∼2.6 for 34 data points in the worst case of the *Swift* UVM2 data set. In the latter case, the data may be somewhat compromised by the fact that the peak of the source PSF was affected by coincidence losses in the first two exposures, although we attempted to circumvent this difficulty by using annular apertures. The remaining statistically significant deviations from χ^2/dof of unity can be traced to large systematic outliers and well-known correlated systematic errors in the photometry. In addition, as we discuss in detail below, the PAIRITEL data show some evidence for a small but nonzero component of blended light which may be due to the lens itself. We therefore conclude that the microlensing model provides a good representation of the data.

Accepting the microlensing interpretation, we then refit the microlensing model. We use an iterative procedure to remove large outliers from the CBA data ($\gtrsim 3\,\sigma$ for CBA V and $\gtrsim 3.5\,\sigma$ for CBA clear) and renormalize the uncertainties in each data set by a constant factor to force $\chi^2/{\rm dof} = 1$, except for the UV data, for which we instead add a constant 0.03 mag uncertainty in quadrature. To provide limits on the magnitude of any contribution of light from the lens itself, we now allow for two parameters for each of the eight separate observatory/filter combinations: the flux of the lensed source and a free term for any flux that is blended with the source but is not microlensed. This model has $3 + 2 \times 8 = 19$ parameters. We find $t_{\rm E} = 7.19 \pm 0.03$ days, $u_0 = 0.0237 \pm 0.0007$, and $t_0 = 4039.899 \pm 0.003$. This timescale is unexpectedly short; for a typical lens velocity relative to the observer-source line of sight of $v_\perp \sim 70$ km s^{-1}, a lens mass of $M \sim 0.3\,M_\odot$, and a lens distance of $D_L \sim 500$ pc, one would expect $t_{\rm E} \sim 20$ days. This implies that the lens is moving fast, is of low mass, is very close to the source or observer, or some combination of these.

In order to provide more quantitative constraints on the nature of the lens, we perform a Bayesian analysis. We adopt priors for the parameters of microlensing events expected toward the GSC 3656−1328 line of sight generated from a Galactic model which includes double exponential thin and thick disks, an exponential distribution of dust in the vertical direction, and a mass function

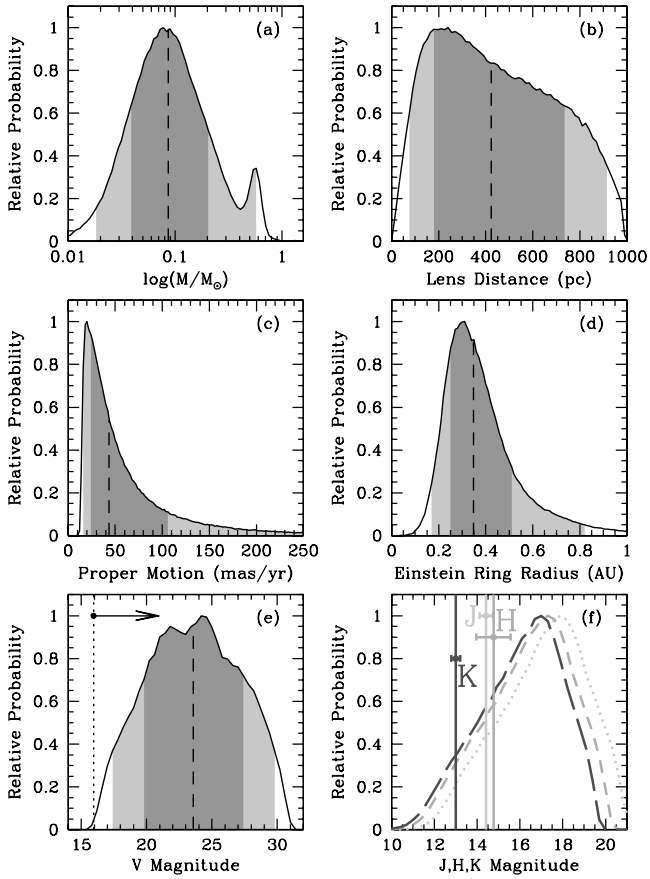

FIG. 3.—Bayesian probability densities for the properties of the lens star giving rise to the microlensing event seen in GSC 3656−1328. These distributions are derived assuming priors obtained from models of the mass, velocity, and density distributions of stars in the thin and thick disks and include constraints on the proper motion of the source and timescale of the microlensing event, as well as limits on the proper motion and *V*-band magnitude of the lens as derived from the light curve. See the text for details. The panels show the probabilities for (*a*) the lens mass, (*b*) the lens distance, (*c*) the lens proper motion, (*d*) the Einstein ring radius of the lens, (*e*) the *V* magnitude of the lens, and (*f*) the *J* (*dotted line*), *H* (*short-dashed line*), and K_s (*long-dashed line*) magnitudes of the lens. In (*a*)–(*e*), the dashed line shows the medians of the distributions, and the dark- and light-shaded regions encompass the 68.3% and 95.4% confidence intervals, respectively. In (*e*) the dotted line shows the 95% confidence level upper limit on the *V*-band flux from the lens. In (*f*) the solid lines show the measured blend fluxes from the JHK_s light curves. The points show the same along with associated uncertainties; the abscissa values are arbitrary. [*See the electronic edition of the Journal for a color version of this figure.*]

of lenses including stars, brown dwarfs, and remnants. We include constraints derived from the measured proper motion of the source, as well as constraints from the analysis of the light curve. These latter constraints include the measurement of the timescale of the event, as well as limits on the angular size of the source in units of the Einstein ring radius, and the flux of the lens. Details of the Bayesian analysis, including information about the model assumptions and parameters, as well as the observational constraints, are provided in Appendix B.

Figure 3 shows the Bayesian probability densities for the properties of the lens star giving rise to the microlensing event seen in GSC 3656−1328. Shown are the results for the lens mass, distance, relative lens-source proper motion μ, Einstein ring radius $R_{\rm E}$, and the *V*, *J*, *H*, and K_s magnitudes of the lens, assuming it is a main-sequence star. The median and 68.3% confidence intervals are $\log(M/M_\odot) = -1.06^{+0.39}_{-0.35}$, $D_L = 420^{+320}_{-250}$ pc, $\mu = 43^{+63}_{-21}$ mas yr^{-1}, and $R_{\rm E} = 0.35^{+0.17}_{-0.10}$ AU. There is an ~49% probability that the lens is a main-sequence star, an ~46% probability that the lens is a brown dwarf, and an ~5% probability that the lens is a white dwarf. The probability that the lens is a neutron star or black hole is negligible. The velocity of the lens relative to the observer-source line of sight is $v_\perp = 84^{+41}_{-25}$ km s^{-1}, indicating that it is probably a member of the thick disk. Thus, the most likely scenario for the lens is that it is a low-mass star or brown dwarf in the thick disk with a mass near the hydrogen-burning limit. The proper motion is likely to be quite high, with $\mu \gtrsim 16$ mas yr^{-1} at the 95% confidence level. The apparent magnitudes of the lens, assuming it is a main-sequence star, are $V = 23.6^{+3.9}_{-3.8}$, $J = 17.3^{+1.9}_{-2.5}$, $H = 16.6^{+1.8}_{-2.4}$, and $K_s = 16.2^{+1.7}_{-2.4}$. Therefore, light from the lens may be directly detectable in a few years, when it has separated from the source, using high-resolution, near-infrared imaging.

Given that the source is quite luminous and the lens likely to be of relatively low mass, one would generally expect any blended light due to the microlens to be very small by comparison. Indeed, the measured blend flux values for the CBA *I*, CBA *V*, and *Swift* M2 data sets are all consistent with zero and less than 2% of the source flux. For the ASAS *I* and *V* data sets, the blending is significant, but as discussed previously, the ASAS photometric aperture is known to contain light from nearby stars that are unresolved by ASAS but resolved by the CBA data. Surprisingly, we find evidence for significant blended light in the *J* and K_s bands and marginal evidence in the *H* band. Specifically, we find blend magnitudes of $(J)_B = 14.41 \pm 0.31$, $(H)_B = 14.76 \pm 0.81$, and $(K_s)_B = 13.00 \pm 0.20$. The color and magnitude of this blended light are roughly consistent with that of a mid-to-late *M* dwarf located ~100 pc away. Although it is a priori unlikely that the lens would be sufficiently close that its light could be detectable against such a bright source, the short timescale of the event already argues for a somewhat more nearby lens, making the detection of blended light more plausible. Indeed, as can be seen from Figure 3, even ignoring any potential constraints from the JHK_s flux of the lens, there is a small but nonnegligible probability for the flux from the lens to be as large as the measured blended light.

If we assume that the blended light is indeed due to the lens, we can include this information in the Bayesian analysis to provide much stronger constraints on the properties of the lens (Bennett et al. 2007). Figure 4 shows the resulting probability densities. We find that the mass, distance, and proper motion are more tightly constrained, $\log(M/M_\odot) = -0.79^{+0.19}_{-0.15}$, $D_L = 130^{+62}_{-48}$ pc, and $\mu = 150^{+24}_{-20}$ mas yr^{-1}, whereas the constraints on the Einstein ring radius are quite similar ($R_{\rm E} = 0.39^{+0.17}_{-0.12}$ AU). The lens apparent magnitudes are $V = 20.2^{+1.5}_{-1.4}$, $J = 14.5^{+0.21}_{-0.18}$, $H = 13.9^{+0.20}_{-0.17}$, and $K = 13.5^{+0.21}_{-0.18}$. We note that the median posterior value of the K_s apparent magnitude differs substantially from the input constraint due to the strong prior that the lens be more distant and less massive, and hence fainter.

If the blended light is real and indeed due to the lens, the lens must be fairly nearby and have a high proper motion ($\mu \gtrsim 110$ mas yr^{-1} at 95% confidence), and so should be resolved from the source in a few years. However, there are caveats. The IR data in this event (as well as other data taken by PAIRITEL) show evidence for low-level systematic errors at the few percent level that are correlated on the timescale of several days. Furthermore, the early IR data were taken when the source was sufficiently bright that nonlinearity may be important. Either of these systematic effects could easily give rise to a spurious blending signal. Regardless, the hypothesis that the lens is nearby should be testable in the near future with high-resolution IR imaging. A measurement of the lens proper motion and relative lens-source parallax, when combined with the timescale of the microlensing event,

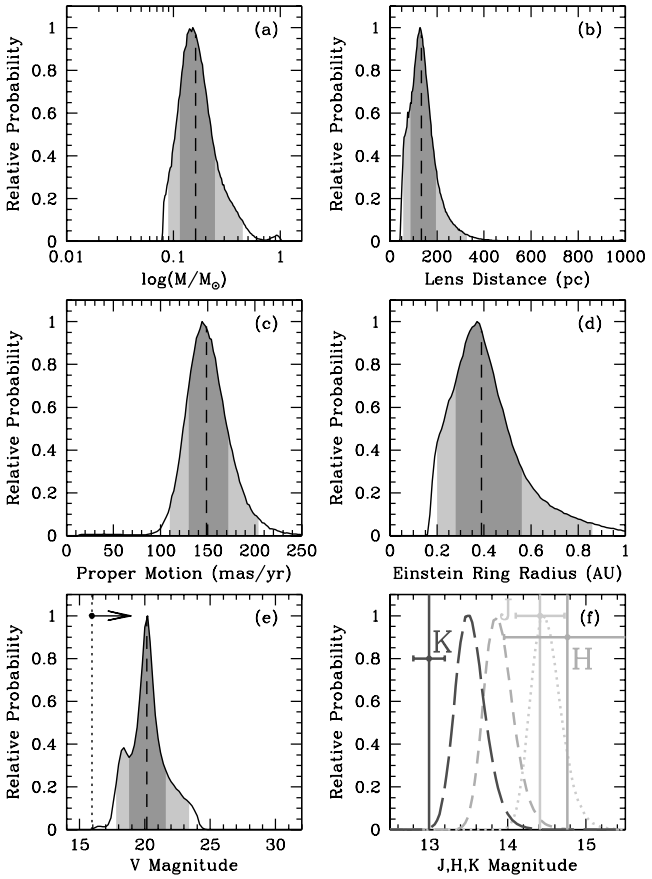

FIG. 4.—Same as Fig. 3, but assuming that the blend fluxes measured in the JHK_s light curves are real and correspond to flux from the lens. This constrains the mass and distance to the lens and implies that the lens is relatively nearby with a large proper motion of $\mu \gtrsim 100$ mas yr^{-1}. Note the greatly compressed scale in (f) as compared to Fig. 3. [*See the electronic edition of the Journal for a color version of this figure.*]

would allow for measurement of the lens mass (Refsdal 1964; Paczynski 1995).

The rate Γ of microlensing events of a single source lying at a distance D by a uniform population of perturbers of number density n is (Paczyński 1986)

$$\Gamma = \frac{\pi}{2} G^{1/2} n \left\langle m^{1/2} \right\rangle \frac{\langle v_\perp \rangle}{c} D^{3/2}, \quad (1)$$

where G is the gravitational constant, $\langle m^{1/2} \rangle$ is the mean square-root mass of the perturbers, and $\langle v_\perp \rangle$ is their mean velocity relative to the observer-source line of sight. Adopting $\langle m^{1/2} \rangle = (0.5\ M_\odot)^{1/2}$, $\langle v_\perp \rangle = 55$ km s^{-1}, $n = 0.1$ pc^{-3}, and $D = 1$ kpc, this yields $\Gamma = 0.043$ Myr^{-1}. Since there are of order 2 million stars in the Tycho-2 catalog, and noting that the source (GSC 3656−1328) is near the brightness limit of this catalog, one would expect one microlensing event of a Tycho-2 star every ∼12 yr. This crude estimate is in rough agreement with the more detailed calculations of Han (2007), who finds a rate of one event every ∼6 yr for stars brighter than $V = 12$. Thus, at first sight, the detection of a microlensing event with a source star with $V \sim 12$ seems very plausible, given that amateur and professional observers have been combing the skies for comets for almost 40 years. However, it is unlikely that this microlensing event would have stimulated enough interest to generate the high-quality follow-up observations that made a convincing case for microlensing if it had not been magnified by at least $A > 10$. Such events are a factor $A^{-1} = 1/10$ less likely to occur. Furthermore, the fraction of the event duration when the source is magnified by $>A$ is also $\sim A^{-1}$. Taking these factors into account, we were probably lucky to observe such a microlensing event, but perhaps not unreasonably so.

4. DISCUSSION

The above calculation and the more detailed study by Han (2007) show that the event rate for sources at ∼1 kpc would be quite small, even with a more thorough and aggressive search procedure that detected essentially all lenses that come within 1 Einstein radius ($A \sim 1.34$) of the source. However, if the search could be extended from 1 to 4 kpc, then the event rate would be increased by $4^{7/2} = 128$ times, to roughly 8 yr^{-1}. That is, we obtain $D^{3/2}$ from equation (1) and D^2 from the larger volume probed (since viable targets are effectively confined to the two-dimensional structure of the Galactic plane). Such a survey would enable a probe of the matter distribution near the Sun that was equally sensitive to dark and luminous objects (see also Di Stefano 2005). It would also bring microlensing planet searches, which have been successful at detecting some novel planets against distant sources in the Galactic bulge (Bond et al. 2004; Udalski et al. 2005; Beaulieu et al. 2006; Gould et al. 2006), nearer to home (Di Stefano 2008a, 2008b; Di Stefano & Night 2008).

In order to provide an illustrative example of the planet discovery potential of such nearby microlensing events, we determine what the sensitivity of this microlensing event to planetary companions would have been had it been discovered well before peak. Specifically, we create a fake data set and then determine the planet detection sensitivity of this data set using the methods outlined in Dong et al. (2006). We assume that before JD′ = 4034.0, the event was sampled at a rate of one point per day. For the time intervals of $4034.0 \leq \mathrm{JD}' \leq 4037.0$ and $4046.0 \leq \mathrm{JD}' \leq 4080.0$, we assume one point every 30 minutes, and over the peak, $4037.0 \leq \mathrm{HJD}' \leq 4046.0$, we assume one point per minute. We assume a photometric uncertainty of 0.4% for each data point. These assumptions are reasonable given the large number of amateur and professional northern telescopes that are available to follow these events, as well as the bright apparent magnitude of the event. We then determine the planet detection sensitivity of this simulated data for planet/star mass ratios of $q = 10^{-3}$, $10^{-3.5}$, 10^{-4}, $10^{-4.5}$, and 10^{-5}.

The finite size of the source will begin to suppress perturbations for mass ratios such that $\sqrt{q} \sim \rho_*$, where $\rho_* \equiv \theta_*/\theta_{\rm E}$ is the angular size of the source θ_* in units of the angular Einstein ring radius $\theta_{\rm E}$. The Bayesian analysis presented in § 3 predicts a source size in units of the Einstein ring radius of $\rho \simeq 10^{-2}$, and therefore we expect perturbations from mass ratios of $\lesssim 10^{-4}$ to be suppressed by finite source effects. For the lowest mass ratio we consider, $q = 10^{-5}$, these suppressions are significant, and so we include finite source effects assuming $\rho = 10^{-2}$.

Figure 5 shows the projected positions of the planet relative to the position of the primary, where the planet would be detected with $\Delta\chi^2 \geq 160$. Here the two components of the position of the planet (b_x, b_y) are in units of $R_{\rm E}$, and b_x is parallel to the direction of the relative source-lens proper motion, such that the source moves from left to right relative to the primary along a trajectory with $b_y = u_0 = 0.0237$. The Bayesian analysis predicts a primary mass of $M \sim 0.1\ M_\odot$ and $R_{\rm E} \sim 0.4$ AU. Therefore, a Neptune-mass ($q \sim 10^{-3.3}$) planet would be detectable over a range of projected separations of ∼0.2−1 AU, and planets with masses as low as $\sim 0.3\ M_\oplus$ ($q \sim 10^{-5}$) would be detectable for some separations near the Einstein ring radius (∼0.4 AU).

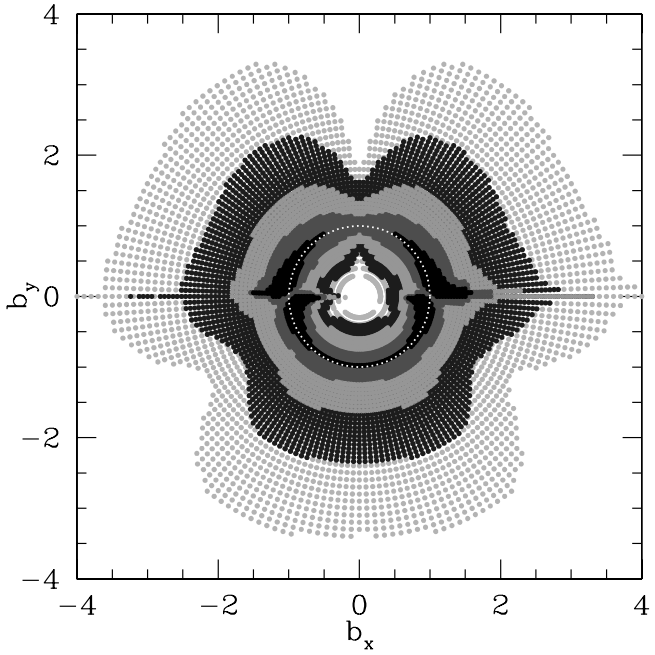

FIG. 5.—Planetary detection efficiency for simulated data of the GSC 3656−1328 microlensing event, assuming that it was monitored densely over the peak with a photometric precision of ∼0.4%. The points show the projected coordinates of the planet (b_x, b_y) relative to the position of the primary star, at which the planet would be detected with $\Delta\chi^2 \geq 160$. Here b_x is parallel to the direction of the relative source-lens proper motion. The projected positions are in units of the Einstein ring radius of the primary; the most likely value for the Einstein radius is ∼0.4 AU. The shades of gray correspond to planet/star mass ratios of 10^{-3} (*outer portion*), $10^{-3.5}$, 10^{-4}, $10^{-4.5}$, and 10^{-5} (*inner portion*). A mass ratio of $\sim 10^{-4.5}$ corresponds to an Earth-mass companion for the most likely primary mass of $\sim 0.1\ M_\odot$. [*See the electronic edition of the Journal for a color version of this figure.*]

Identifying all of the microlensing events within 4 kpc would require an all-sky (or at least all-Galactic-plane) survey that reached a flux level roughly 60 times fainter than GSC 3656−1328, or $V \sim 16$, to compensate partly for the greater distance and partly for the increased interstellar extinction toward more distant targets. It would be straightforward to place 120 10 cm lenses, each backed by a 20 megapixel camera with 7″ pixels, on one single-axis mount, and so continuously monitor to the required depth the 10,000 deg^2 that are within 60° of the zenith at any given time. To cover the whole Galactic plane would require two such devices, one in each hemisphere. Such "fly's eye" telescopes would have heritage in ongoing experiments such as ASAS (Pojmański 2004) and SuperWASP (Pollacco et al. 2006) and could be considered the "next generation" successors to these experiments. In addition to detecting nearby microlensing events, these telescopes would have a very large number of other science applications. Although the technical and survey requirements for each application are fairly distinct, these telescopes could in principle be used to detect thousands of planets as they transit their host star, rapidly identify gamma-ray burst afterglows (in plenty of time to alert gamma-ray satellites—the reverse of the usual procedure), and provide several days' advance warning for Tunguska-size meteors that are expected to hit the Earth of order once per century with 10 megaton impacts (Paczynski 2006).

We thank Weidong Li for assistance with the *Swift* UVOT data; Eric Ford for help with MCMC; Kris Stanek for reminding us about Paczynski (1995); Martin Dominik, Pascal Fouqué, and Stefan Dieters for enlightening discussions; and Arto Oksanen, Becky Enoch, Dave Messier, Arne Henden, and Tut Campbell for contributions of data. We would like to thank the referee, J. P. Beaulieu, for a helpful report. The Peters Automated Infrared Imaging Telescope (PAIRITEL) is operated by the Smithsonian Astrophysical Observatory (SAO) and was made possible by a grant from the Harvard University Milton Fund, the camera loan from the University of Virginia, and the continued support of the SAO and UC Berkeley. The PAIRITEL project is further supported by NASA/*Swift* Guest Investigator Grant No. NNG06GH50G. We thank M. Skrutskie for his continued support of the PAIRITEL project. We acknowledge the use of public data from the *Swift* data archive. A. G. and S. D. were supported by NSF grant AST 042758. C. B. would like to acknowledge support from the Harvard Origins of Life Initiative.

APPENDIX A

PROPERTIES OF THE SOURCE STAR

GSC 3656−1328 (TYC 3656−1328−1) has a spectral type of A0 V–A1 V and is located in the constellation Cassiopeia ($\alpha = 00^{\rm h}09^{\rm m}21.99^{\rm s}$, $\delta = +54^\circ 39' 43.8''$ [J2000.0]; $l = 116.8158^\circ$, $b = -7.7092^\circ$). The Tycho catalog (Høg et al. 2000) gives a proper motion of $\mu_\alpha = -2.0 \pm 2.8$, $\mu_\delta = -6.1 \pm 2.7$ mas yr^{-1}, and $V_T = 11.387 \pm 0.076$ and $B_T = 11.507 \pm 0.054$. We convert the latter to $V = 11.376 \pm 0.076$ and $B = 11.478 \pm 0.054$ using the standard *Hipparcos* (ESA 1997) transformation. This V magnitude is consistent with our more precise inferred value of $V = 11.39 \pm 0.01$, which we adopt here. The color of $B - V = 0.102 \pm 0.093$ is consistent with, but less accurate than, the value of $B - V = 0.19 \pm 0.01$ measured by Mikolajewski et al. (2006b) when GSC 3656−1328 was ∼1 mag above baseline. Because we see no evidence for chromaticity, we adopt the more precise determination of Mikolajewski et al. (2006b) as the baseline color of the source.

We estimate the distance to the source using its color and magnitude, assuming a dereddened color and magnitude appropriate for its A0 V–A1 V spectral type inferred by Mikolajewski et al. (2006a). Adopting the spectral type/color calibration of Kenyon & Hartmann (1995), we estimate $E(B - V) = 0.16$–0.19, and assuming $R_V = 3.1$, we estimate a V-band extinction of $A_V = 0.5$–0.6. The apparent V magnitude then implies a distance of $D = 960$–1070 pc. For definiteness, we adopt $A_V = 0.6$ and $D = 1$ kpc. Using the observed $V - K_s$ of the source at baseline gives reasonably consistent results; however, uncertainties about the possible presence of systematics in the PAIRITEL data, as well as potential contamination from light due to the lens itself, make these results less secure despite the longer wavelength baseline.

We estimate the angular size of the source to be $\theta_* \simeq 10\ \mu$as, based on the dereddened $(V - K)_0$ color and V_0 magnitude of the source and the color–surface brightness relations of Kervella et al. (2004). The uncertainty in this estimate is not important for our purposes, but it is roughly a few percent due to the uncertainty in $(V - K)_0$ and V_0.

APPENDIX B

BAYESIAN CONSTRAINTS ON THE LENS STAR PROPERTIES

In order to provide constraints on the properties of the lens giving rise to the microlensing event in GSC 3656−1328, we perform a Bayesian analysis, which naturally accounts for priors on the expected populations of microlensing events toward the line of sight of GSC 3656−1328, as well as the observed constraints from the light curve and additional (external) information. Our analysis is similar to that done for other microlensing events (see, e.g., Yoo et al. 2004; Dong et al. 2006; Dominik 2006; Bennett et al. 2007); however, there are some particular nuances in the analysis of this particular event that motivate an in-depth discussion.

We construct prior distributions of microlensing event parameters using simple models of the mass, density, and velocity distributions of the lens stars. We adopt double exponential models for the thin and thick disks. Our thin-disk model is the same as that used by Han & Gould (1995, 2003) with a scale length of 3.5 kpc and scale height of 325 pc, and our thick-disk model has the same scale length but a scale height of 1 kpc. We adopt a Chabrier (2003) lognormal mass function with a peak at $M = 0.079\,M_\odot$ and a width of 0.69 dex for stars with $M \leq M_\odot$ and the present-day mass function as measured by Reid et al. (2002) with a logarithmic slope of $\alpha = -4.2$ for stars with $M \geq M_\odot$. We add remnants following Gould (2000). We adopt Gaussian distributions for the lens velocities that are independent of position along the line of sight. These have means in the $\boldsymbol{U}, \boldsymbol{V}, \boldsymbol{W}$ directions of $(\bar{v}_{\boldsymbol{U}}, \bar{v}_{\boldsymbol{V}}, \bar{v}_{\boldsymbol{W}}) = (0, 214, 0)$ km s^{-1} and one-dimensional velocity dispersions of $(\sigma_{\boldsymbol{U}}, \sigma_{\boldsymbol{V}}, \sigma_{\boldsymbol{W}}) = (35, 28, 35)$ km s^{-1} for the thin disk and twice this for the thick disk.

In the absence of external constraints, the likelihood of a given lens mass, distance, and velocity is just the contribution to the microlensing event rate, which for fixed-source proper motion and distance is given by

$$\mathcal{L}_\Gamma \propto \frac{R_{\rm E} v_\perp}{M} \left(\rho_1 G_{\boldsymbol{U},1} G_{\boldsymbol{V},1} G_{\boldsymbol{W},1} + \rho_2 G_{\boldsymbol{U},2} G_{\boldsymbol{V},2} G_{\boldsymbol{W},2}\right) f_X \left(\frac{dn}{dM}\right)_X . \tag{B1}$$

Here subscripts "1" and "2" are quantities for the thin and thick disks, respectively, ρ is the mass density at the position of the lens, and G is the exponential velocity distribution. For example,

$$G_{\boldsymbol{U},1} = \frac{1}{\sqrt{2\pi}\sigma_{\boldsymbol{U},1}} \exp\left(\frac{-[v_{\boldsymbol{U}} - \bar{v}_{\boldsymbol{U}}]^2}{2\sigma^2_{\boldsymbol{U},1}}\right), \tag{B2}$$

and similarly for the other distributions. The (normalized) mass function of each population of lenses (stars, brown dwarfs, etc.) is given by $(dn/dM)_X$, and f_X is the relative contribution to the number density from each type of lens. These are 66.3%, 29.7%, 3.4%, and 0.5% for main-sequence stars + brown dwarfs, white dwarfs, neutron stars, and black holes, respectively. The lens velocity relative to the observer-source line of sight is given by

$$\boldsymbol{v}_\perp = \boldsymbol{v}_{L,\perp} - \boldsymbol{v}_{O,\perp}\left(1 - \frac{D_L}{D_S}\right) - \boldsymbol{v}_{S,\perp}\frac{D_L}{D_S}. \tag{B3}$$

Here $\boldsymbol{v}_{L,\perp}$, $\boldsymbol{v}_{S,\perp}$, and $\boldsymbol{v}_{O,\perp}$ are the projected velocities of the lens and the observer perpendicular to observer-source line of sight, where $\boldsymbol{v}_{O,\perp}$ accounts for both the velocity of the Sun and the velocity of the Earth at the time of the event.

The projected velocity of the source is just its proper motion times its distance, both of which are constrained (Appendix A). We account for these constraints by including a term in the overall likelihood of the form

$$\mathcal{L}_\mu \propto \exp\left\{-\frac{1}{2}\left(\frac{\mu_\alpha - [-2.0\ {\rm mas\ yr^{-1}}]}{2.8\ {\rm mas\ yr^{-1}}}\right)^2\right\} \exp\left\{-\frac{1}{2}\left(\frac{\mu_\delta - [-6.1\ {\rm mas\ yr^{-1}}]}{2.7\ {\rm mas\ yr^{-1}}}\right)^2\right\}. \tag{B4}$$

We fix the lens distance at $D_S = 1$ kpc but test the effects of changing this value.

We can account for the constraints from the light curve by including additional likelihood terms. We consider constraints from the fitted timescale of the event, the blend flux in the V band, the apparent lack of finite source effects, and, in some cases, the blend fluxes in the JHK_s bands. The constraint on the timescale takes the form

$$\mathcal{L}_{t_{\rm E}} \propto \exp\left[-\frac{1}{2}\left(\frac{t_{\rm E} - 7.19\ {\rm days}}{0.03\ {\rm days}}\right)^2\right]. \tag{B5}$$

The light curve exhibits marginal evidence of finite source effects, with $\rho_* = 0.032$ and an upper limit of $\rho_* < 0.044$ at the 3 σ level. We note that from the observed color and flux of the source, $\theta_* = 10$ μas (see Appendix A), this limit on ρ_* constrains the source-lens relative proper motion to be $\mu = \theta_{\rm E}/t_{\rm E} > 10$ mas yr^{-1}. Since the angular speed of the source is 6.4 ± 3.9 mas yr^{-1} and that of the lens is expected to be similar, this range is plausible. This also implies that the lack of finite source effects does not provide a strong constraint on the properties of the lens, other than ruling out lenses that are very close to the source. Nevertheless, we include this constraint on ρ_* from

the light curve by first determining $\Delta\chi^2_{\rm fs}(\rho_*)$, the change in χ^2 from the best-fit point-source model as a function of ρ_*, when allowing all the other parameters to vary. The likelihood of a particular ρ_* then takes the form

$$\mathcal{L}_{\rho_*} \propto \exp\left[-\Delta\chi^2_{\rm fs}(\rho_*)/2\right]. \tag{B6}$$

We also consider constraints on the flux of the lens arising from measurements of (or limits on) the blend flux from the analysis of the light curve. We assume that brown dwarfs and remnants are dark. For main-sequence lenses we adopt mass-luminosity relations from the solar-metallicity, 1 Gyr isochrone of Siess et al. (2000), which in turn adopt empirical transformations from effective temperature to standard filter luminosities from Kenyon & Hartmann (1995). We apply a (small) correction to convert the standard Bessell & Brett (1988) *JHK* magnitudes given in these isochrones to the 2MASS system.[19] To estimate the extinction along the line of sight to the lens, we assume a vertically exponential dust disk with a scale height of 120 pc, normalized such that the total extinction to the source is $A_V = 0.6$ (see Appendix A). We use a standard extinction law ($R_V = 3.1$) to convert to other bandpasses. We then apply the constraints on the lens fluxes from the light curve, assuming that the blend flux is entirely due to the lens star. For the V band the strongest constraint on the blend flux is $f_V = 0.00058 \pm 0.00181$, where the units are such that $f_V = 1$ corresponds to a $V = 10$ star. If we are considering only the constraint from the V-band flux, then the likelihood is simply

$$\mathcal{L}_{\rm lc} \propto \exp\left(-\Delta\chi^2_{\rm lc}/2\right), \tag{B7}$$

where $\Delta\chi^2 = \left[(f_V - f_{V,\rm model})/\sigma_V\right]^2$, $\sigma_V = 0.00181$, and $f_{V,\rm model}$ is the V-band flux of the lens predicted by the model. We can also include constraints from the blend fluxes in the infrared. The measured blend fluxes f_J, f_H, f_{K_s} in the JHK_s bands are given in § 3. Since these fluxes are correlated with each other and with the V-band flux within the microlensing fit, we must adopt a somewhat more sophisticated approach. We first construct the vector $\Delta\boldsymbol{a} = (f_V - f_{V,\rm model},\ f_J - f_{J,\rm model},\ f_H - f_{H,\rm model},\ f_{K_s} - f_{K_s,\rm model})$, where $f_{V,\rm model}$, $f_{J,\rm model}$, . . . are the model fluxes. From the microlensing fit to the light curve, we can also construct the covariance matrix $\mathcal{C}$ for the four blend-flux parameters. The difference in χ^2 between the fluxes predicted by the model and the measured fluxes is

$$\Delta\chi^2_{\rm lc} = \sum_{i=1}^{4}\sum_{j=1}^{4} \Delta a_i \mathcal{B}_{i,j} \Delta a_j, \tag{B8}$$

where $\mathcal{B} \equiv \mathcal{C}^{-1}$. The likelihood is then determined using equation (B7), as before.

Finally, the likelihood of a particular parameter combination is given by

$$\mathcal{L}_{\rm tot} = \mathcal{L}_\Gamma \mathcal{L}_\mu \mathcal{L}_{t_{\rm E}} \mathcal{L}_{\rho_*} \mathcal{L}_{\rm lc}. \tag{B9}$$

We construct a posteriori probability densities using the Markov chain Monte Carlo method. We first randomly choose values for the lens mass, distance, and $(\boldsymbol{U}, \boldsymbol{V}, \boldsymbol{W})$ velocity components $v_{\boldsymbol{U}}, v_{\boldsymbol{V}}, v_{\boldsymbol{W}}$ over a range of parameter space that is broad in comparison to the posterior probability distributions. We also randomly choose whether the lens is a main-sequence star, brown dwarf, white dwarf, neutron star, or black hole. Finally, we choose a random value for the two components of the proper motion of the source. We evaluate the relative likelihood of this parameter combination using equation (B9). We then randomly move to another point in the parameter space of lens mass, distance, velocity, and source proper motion and evaluate the likelihood of this new parameter combination. We step in parameter space by adding to each of the parameters a random value drawn from a Gaussian distribution with zero mean and dispersion chosen to efficiently sample the likelihood surface. Specifically, these dispersions are 0.043 dex in $\log(M/M_\odot)$ for M, 148 pc for D_L, $\sigma_{\boldsymbol{U}}, \sigma_{\boldsymbol{V}}, \sigma_{\boldsymbol{W}}$ for the lens velocities, and 2.7 mas yr^{-1} for the two components of the source proper motion. If the ratio of the likelihood of the new parameter combination to the old combination is greater than unity, we take the step. Otherwise, we draw a random number between 0 and 1. If this number is less than this ratio of likelihoods, we take the step; otherwise, it is rejected. After discarding the first 10^4 steps, we record every 10^3 steps until we form a chain of 10^5 points. We form 10 such chains, each starting from different initial conditions, and calculate the Gelman & Rubin (1992) R-statistic. This is within 0.2% of unity for each parameter, indicating that the chains are well mixed and converged. We then merge the chains and use the result for the final probability distributions.

We also test the effects of changing the source distance by ± 100 pc and the V-band extinction to the source by ± 0.2 mag. We find that the medians of the probability distributions change by $\lesssim 5\%$ for all of the parameters of interest.

[19] See http://www.astro.caltech.edu/~jmc/2mass/v3/transformations/.

REFERENCES

Afonso, C., et al. 2006, A&A, 450, 233
Alcock, C., et al. 1993, Nature, 365, 621
———. 1996, ApJ, 461, 84
———. 1997, ApJ, 491, L11
———. 2000, ApJ, 542, 281
———. 2001, Nature, 414, 617
Ansari, R., et al. 1995, A&A, 299, L21
Aubourg, E., et al. 1993, Nature, 365, 623
Beaulieu, J. P., et al. 1995, A&A, 299, 168
———. 2006, Nature, 439, 437
Bennett, D. P., Anderson, J., & Gaudi, B. S. 2007, ApJ, 660, 781
Bessell, M. S., & Brett, J. M. 1988, PASP, 100, 1134
Bloom, J. S., Starr, D. L., Blake, C. H., Skrutskie, M. F., & Falco, E. E. 2006, in ASP Conf. Ser. 351, Astronomical Data Analysis Software and Systems XV, ed. C. Gabriel et al. (San Francisco: ASP), 751
Bond, I. A., et al. 2004, ApJ, 606, L155
Burrows, D. N., et al. 2005, Space Sci. Rev., 120, 165
Calchi Novati, S., et al. 2005, A&A, 443, 911
Chabrier, G. 2003, PASP, 115, 763
Chwolson, O. 1924, Astron. Nachr., 221, 329
Colley, W. N., & Gott, J. R. I. 1995, ApJ, 452, 82
Cook, K. H., et al. 1995, in IAU Colloq. 155, Astrophysical Applications of Stellar Pulsation, ed. R. S. Stobie & P. A. Whitelock (ASP Conf. Ser. 83; San Francisco: ASP), 221

de Jong, J. T. A., et al. 2004, A&A, 417, 461
della Valle, M. 1994, A&A, 287, L31
della Valle, M., & Livio, M. 1996, ApJ, 457, L77
Derue, F., et al. 2001, A&A, 373, 126
Di Stefano, R. 2005, ApJ, submitted (astro-ph/0511633)
———. 2008a, ApJ, in press (arXiv: 0712.3558)
———. 2008b, ApJ, submitted (arXiv: 0801.1511)
Di Stefano, R., & Night, C. 2008, ApJ, submitted (arXiv: 0801.1510)
Dominik, M. 2006, MNRAS, 367, 669
Dong, S., et al. 2006, ApJ, 642, 842
Eddington, A. S. 1920, Space, Time, and Gravitation (Cambridge: Cambridge Univ. Press)
Einstein, A. 1936, Science, 84, 506
ESA. 1997, The *Hipparcos* and Tycho Catalogues (ESA SP-1200; Noordwijk: ESA)
Fukui, A., et al. 2007, ApJ, 670, 423
Gehrels, N., et al. 2004, ApJ, 611, 1005
Gelman, A., & Rubin, D. B. 1992, Statist. Sci., 7, 457
Gould, A. 2000, ApJ, 535, 928
Gould, A., Bennett, D. P., & Alves, D. R. 2004, ApJ, 614, 404
Gould, A., Miralda-Escude, J., & Bahcall, J. N. 1994, ApJ, 423, L105
Gould, A., et al. 2006, ApJ, 644, L37
Hamadache, C., et al. 2006, A&A, 454, 185
Han, C. 2007, ApJ, submitted (arXiv: 0708.1215)
Han, C., & Gould, A. 1995, ApJ, 447, 53
———. 2003, ApJ, 592, 172
Høg, E., et al. 2000, A&A, 355, L27
Kenyon, S. J., & Hartmann, L. 1995, ApJS, 101, 117
Kervella, P., Thévenin, F., Di Folco, E., & Ségransan, D. 2004, A&A, 426, 297
Lasserre, T., et al. 2000, A&A, 355, L39
Liebes, S. 1964, Phys. Rev., 133, 835
Mikolajewski, M., Tomov, T., Niedzielski, A., & Czart, K. 2006a, ATel, 931, 1
Mikolajewski, M., et al. 2006b, ATel, 943, 1
Munari, U., Siviero, A., Tomasella, L., & Valentini, M. 2006, Cent. Bur. Electron. Tel., 718, 1
Nakano, S., Kadota, K., Sakurai, Y., & Waagen, E. 2006, Cent. Bur. Electron. Tel., 712, 1
Nakano, S., & Tago, A. 2006, Cent. Bur. Electron. Tel., 711, 1
Nemiroff, R. J. 1998, ApJ, 509, 39
Nemiroff, R. J., & Rafert, J. B. 1999, PASP, 111, 886
Paczyński, B. 1986, ApJ, 304, 1
———. 1995, Acta Astron., 45, 345
———. 2006, PASP, 118, 1621
Palanque-Delabrouille, N., et al. 1998, A&A, 332, 1
Paulin-Henriksson, S., et al. 2002, ApJ, 576, L121
Pojmański, G. 2004, Astron. Nachr., 325, 553
Pollacco, D. L., et al. 2006, PASP, 118, 1407
Refsdal, S. 1964, MNRAS, 128, 295
Reid, I. N., Gizis, J. E., & Hawley, S. L. 2002, AJ, 124, 2721
Renn, J., Sauer, T., & Stachel, J. 1997, Science, 275, 184
Roming, P. W. A., et al. 2005, Space Sci. Rev., 120, 95
Samus, N. N., & Antipin, S. V. 2006, Cent. Bur. Electron. Tel., 718, 5
Schneider, P., Ehlers, J., & Falco, E. E. 1992, Gravitational Lenses (Berlin: Springer)
Siess, L., Dufour, E., & Forestini, M. 2000, A&A, 358, 593
Skillman, D. R., & Patterson, J. 1993, ApJ, 417, 298
Skrutskie, M. F., et al. 2006, AJ, 131, 1163
Smak, J. 1984, PASP, 96, 5
Smith, M. C. 2003, MNRAS, 343, 1172
Soldner, J. 1804, Berliner Astron. Jahrb. Jahr 1804, 161
Spiegel, D. 2006, ATel, 942, 1
Thomas, C. L., et al. 2005, ApJ, 631, 906
Tisserand, P. 2005, in Semaine de l'Astrophysique Francaise, SF2A-2005, ed. F. Casoli et al. (Les Ulis: EdP Sciences), 569
Tisserand, P., et al. 2007, A&A, 469, 387
Udalski, A., Szymanski, M., Kaluzny, J., Kubiak, M., Krzeminski, W., Mateo, M., Preston, G. W., & Paczynski, B. 1993, Acta Astron., 43, 289
Udalski, A., Zebrun, K., Szymanski, M., Kubiak, M., Pietrzynski, G., Soszynski, I., & Wozniak, P. 2000, Acta Astron., 50, 1
Udalski, A., et al. 2005, ApJ, 628, L109
Uglesich, R. R., Crotts, A. P. S., Baltz, E. A., de Jong, J., Boyle, R. P., & Corbally, C. J. 2004, ApJ, 612, 877
van Paradijs, J. 1985, A&A, 144, 199
Yoo, J., et al. 2004, ApJ, 616, 1204